Journal Pre-proofs

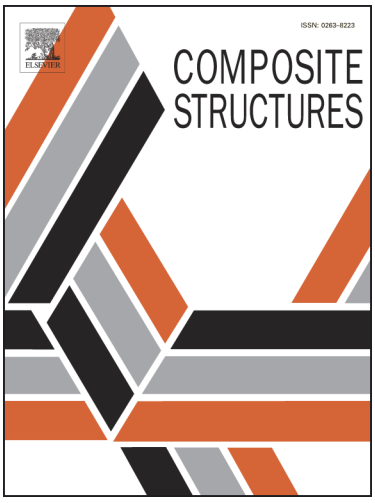


# Mechanical behaviour of composite laminates repaired with a stitched scarf patch

C. Sun, W. Zhao, J. Zhou, M. Altenaiji, W.J. Cantwell, Q.Y. Wang, Z.W. Guan

PII: S0263-8223(20)32854-3
DOI: https://doi.org/10.1016/j.compstruct.2020.112928
Reference: COST 112928

To appear in: *Composite Structures*

Received Date: 18 June 2020
Revised Date: 20 August 2020
Accepted Date: 3 September 2020

Please cite this article as: Sun, C., Zhao, W., Zhou, J., Altenaiji, M., Cantwell, W.J., Wang, Q.Y., Guan, Z.W., Mechanical behaviour of composite laminates repaired with a stitched scarf patch, *Composite Structures* (2020), doi: https://doi.org/10.1016/j.compstruct.2020.112928

# Mechanical behaviour of composite laminates repaired with a stitched scarf patch

C. Sun[a], W. Zhao[b], J. Zhou[b], M. Altenaiji[c], W.J. Cantwell[d], Q.Y. Wang[e] and Z.W. Guan[a,e*]

[a] *School of Engineering, University of Liverpool, Liverpool, L69 3GH, United Kingdom.*

[b] *School of Mechanical Engineering, Xi'an Jiaotong University, Xi'an, 710049, China*

[c] *Technology Innovation Institute, Abu Dhabi, United Arab Emirates.*

[d] *Department of Aerospace Engineering, Khalifa University, Abu Dhabi, United Arab Emirates.*

[e] *School of Mechanical Engineering, Chengdu University, Chengdu, 610100, China*

**Abstract:** In order to increase the service life and maintain the residual strength of damaged composite structures, it is necessary to investigate effective repairing techniques. In this paper, an innovative stitch-reinforced scarf patch is developed in order to reduce the amount of parent material that is removed during the repair. Carbon fibre threads are used to stitch the scarf patch to a damaged carbon fibre laminate via pre-drilled holes. Following stitching, the vacuum resin infusion technique is used to infuse the carbon fibre threads, thereby fixing the patch to the parent part. Here, the effects of varying both the hole diameter and the scarf angle on the load-carrying capacity of the repaired laminates are studied. The tensile strength, strain distribution and failure mechanisms are investigated using the digital image correlation (DIC) technique. The results show that by introducing a 2.5 mm diameter stitching hole, the ultimate tensile strength of repaired laminates related to three scarf angles is increased by up to 20, 27 and 45 % respectively, relative to traditional laminates with an equivalent scarf ratio.

**Keywords:** Woven carbon fibre composite laminate; scarf patch repair; stitching; vacuum resin infusion; digital image correlation (DIC)

*Corresponding author: Z.W. Guan, Email: zguan@liverpool.ac.uk

## 1. Introduction

With the increasing use of composite materials in a broad range of industrial sectors, the sustainability of composite structures has become an important issue. Based on previous experience on maintaining metallic structures, the cost of repairing a damaged part is significantly lower than the cost of replacing the entire component [1]. Therefore, it is necessary to develop low cost repair technologies that offer a high operational efficiency and fully-restored mechanical performance.

At present, two repair methods are widely used, these being a fastened repair and a bonded patch repair. Generally, applications of the fastened repair approach are limited by the laminate thickness, which is typically greater than 8 mm [2]. In addition, it has been noted that the mechanical properties of fasten-repaired laminates are influenced by the bolt arrangement, bolt number and patch material. Kradinov et al. [3] and Her and Shie [4] showed that the ultimate tensile strength of repaired laminates can be increased by increasing the number of bolts and adopting an appropriate arrangement and by using patches with a lower modulus than the parent material. Park et al. [5] and Kang et al. [6] investigated delaminated composite laminates repaired using micro-bolts, and showed that the compressive strength can be restored to 89 % of that of the original laminate. They also showed that a relatively large bolt diameter and a reduced bolt-hole clearance can improve the mechanical performance of the repaired component. In general, the fastened repair method offers the advantage of a high assembly efficiency, low cost and increased durability. However, as with a bolted joint, there is a significant stress concentration around the hole edge in the repaired laminate when subjected to in-plane loading. In addition, the mass of the panel is increased, since most fasteners are made of metals. In some circumstances, an aerodynamic profile cannot be maintained by changing the surface shape of the repaired parts.

Bonded patch repairs can be crudely divided into externally-bonded repairs and scarf repairs. The latter is generally used in primary load-bearing structures and the former is commonly used in secondary load bearing

structures [7]. An externally-bonded repair is a robust and effective approach in composite repair. In this method, the patch can be cured directly on the repaired laminate or the patch can be cured and then bonded on the laminate using an adhesive. The failure strengths associated with the two methods are often similar [8, 9]. Cheng et al. [10] investigated the strain distribution, damage initiation and propagation of damage in externally-bonded repaired composites using infrared thermography. The results show that damage initiates from the edge of the circular patch in the loading direction and then extends towards the central area of the patch. Simultaneously, because of partial loss in the load transfer between the patch and the parent material, a large strain surge was detected at transverse edge of the hole prior to final failure. Kashfuddoja and Ramji [11] investigated single-sided and double-sided externally bonded repairs using 3D DIC technology. They showed that the bonding area at the edges of the circular patch in the loading direction experienced shear and peeling stresses under tensile loading. The failure strength of the double-sided repair was much higher than its single-sided counterpart as expected and both types of repair exhibited similar failure mechanisms [10, 11]. Liu and Wang [1] investigated the effects of adhesive thickness, patch size and patch thickness on the mechanical performance of externally-bonded repairs. They showed that by increasing the patch size and thickness and decreasing the adhesive thickness, the failure strength of the repaired laminates could be improved.

Scarf repair has been widely used in the aerospace field to maintain the original aerodynamic properties of the repaired components. Hamoush [12] studied the failure mechanisms of scarf-repaired laminates by comparing the strain distributions of the original, damaged and repaired laminates. When subjected to tensile loading, high strains were detected in the area close to the transverse edge of the hole in the damaged panel, where failure was observed to initiate. However, the strains in this area were lower in the repaired panel, leading to delayed damage initiation and an increase in ultimate strength. Baig et al. [13] investigated the mechanical performance of composites repaired using pre-formed and prepreg-based scarf patches. The pre-formed patches were made from a cured

prepreg-based material and then bonded onto laminate using an adhesive. The prepreg patches involved placing the prepreg on the repaired area and then curing the stack onto the laminate using the prepreg matrix. The authors noted that larger voids and defects occurred in the pre-formed patches compared to the prepreg patches. For these two types of circular scarf patch, the crack initiates at the longitudinal edge (in the loading direction) of the bonded area and then propagates along the adhesive in a circumferential fashion. With decreasing bond area, the repaired panel exhibited a catastrophic form of failure from the free edge of the repaired laminates. Pinto et al. [14] and Bendemra et al. [15] studied the effect of ply thickness, adhesive thickness, taper angle, stacking sequence and external overlap on the structural performance of repaired composites. Their results showed that with increasing scarf angle, the peel stress along the adhesive interface increased significantly. However, the shear stress along the interface did not vary significantly. This suggests that peel stresses dominate failure initiation and repairs based on a small scarf angle result in a greater restoration of load. Through the use of an extra external patch in scarf-repaired laminates, the residual strength can be restored to up to 70 % of the undamaged laminate strength [14].

Previous research has shown that scarf ratios from 1:20 to 1:60 are considered as the appropriate range in which the residual strength can achieve the design ultimate strength [16]. However, significant amounts of undamaged parent material may need to be removed, which may not be practical in many circumstances. An ideal repair should involve a large scarf angle to limit the removal of parent material, whilst achieving the desired load-bearing capability for the repaired composite. In this paper, an alternative approach combining a traditional scarf patch with carbon fibre stitching is considered. The repairs are achieved using the vacuum-assisted resin transfer moulding technique. A range of scarf angles and stitching hole diameters are investigated and the residual loading bearing response is assessed via in-plane tensile tests combined with the digital image correlation technique.

## 2. Experimental procedure

### 2.1 Sample preparation

A woven XPREG XC130 carbon fibre prepreg from Easy Composites UK was used to fabricate the carbon fibre laminates investigated in this study. Here, five layers of the woven prepreg material (nominal thickness 0.5 mm) were laid up in a closed mold with a stacking sequence of $[0°/90°]_5$ and then cured at 120 °C for 1 hour under a pressure of 2 bar. After curing, samples with dimensions of 250 mm x 100 mm x 2.5 mm were cut from the laminates using a water-jet cutting machine (MAXIEM 1530). Tabs with dimensions of 100 mm x 50 mm x 1.5 mm were used to reinforce the two ends of the repaired panel in the gripping regions. The tabs were based on three layers of prepreg material and manufactured according to the aforementioned cure cycle. The scarf regions on the parent laminates were prepared using a CNC machine (Haas TM1 CNC Mill 2006). Scarf patches were produced by pressing five layers of circular prepreg (with a stacking sequence of $[0°/90°]_5$) in a closed mould, again by adopting the process used to produce the laminates and tabs.

Prior to bonding, the relevant areas on each scarf patch and laminate were polished using P400 abrasive paper and cleaned by acetone. A two-part epoxy resin (ET500 from Easy Composites UK) was used to bond both the tabs and the pre-formed scarf patch to the parent laminate. Effort was made to ensure that the scarf patch and circular repair region were concentric and that the fibres in patch were alignged with those in the repaired laminates. The epoxy adhesive was then cured at room temperature for 24 hours. Prior to the stitching processes, holes, with diameters of 1.5, 2.5 and 3.5 mm, were drilled in the laminates to be repaired. Fig. 1 shows a schematic of a sample before stitching. In Fig. 1(a), the parameter X denotes the outer diameter of the scarf region, with three values being considered here, these being 48, 58 and 68 mm. The scarf angle is defined as the ratio of $t$ / $L$, as shown in Fig. 1(b). Here, scarf ratios equal to 1:8, 1:10 and 1:12 were considered. The positions of the holes and the dimensions of the scarf patches are dependent on the diameter X, as shown in Fig. 1(a). The diameters of the open hole and the scarf patch on the rear side of laminate were maintained constant for all tests, these values being 8

115 mm and 6 mm respectively, as shown in Fig. 1(a). Fig. 1(b) shows a schematic of the cross-section of the repaired

116 region. Here, the green lines correspond to the interfaces between the plies of prepreg material.

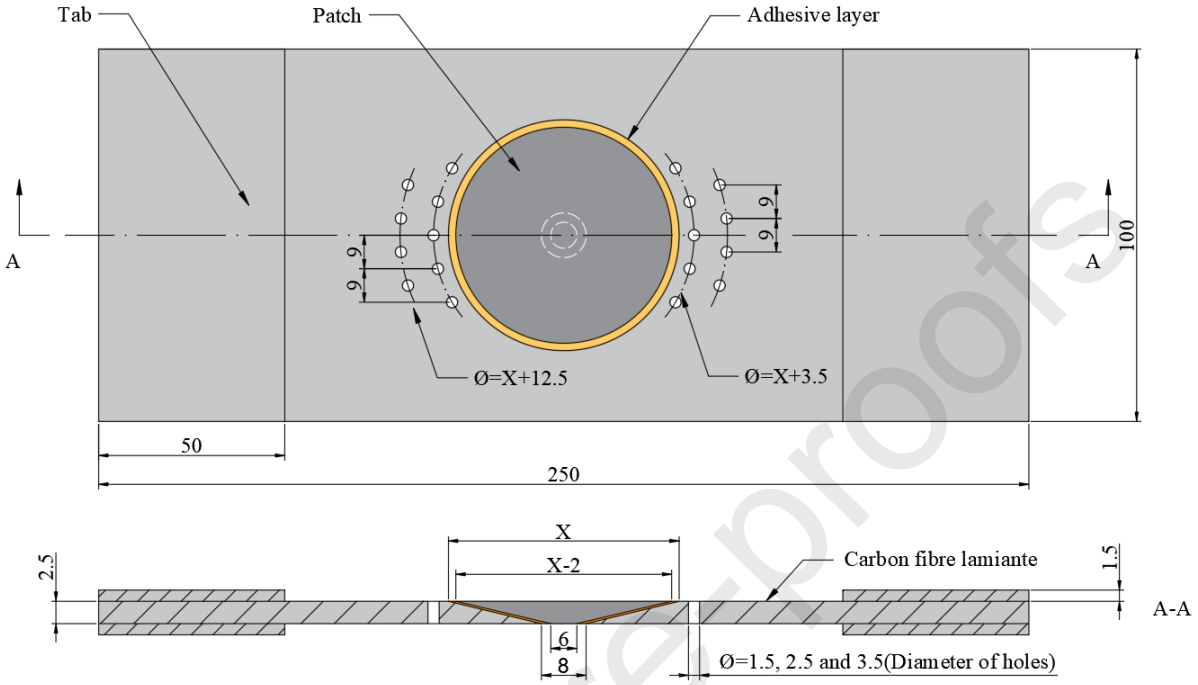


117

118 (a) Dimensions of the sample before the stitching process (Unit: mm)

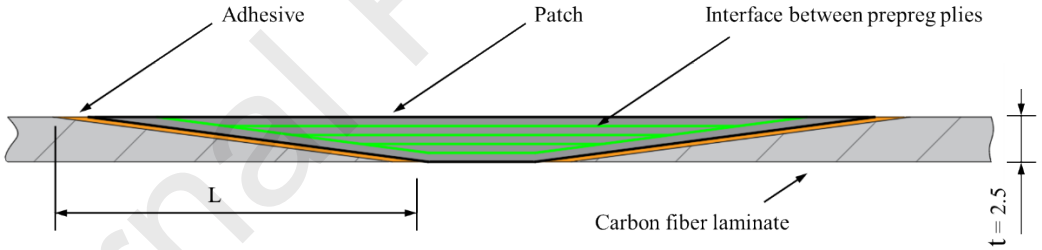


119

120 (b) Cross-section of the bonding area (Unit: mm)

121 Fig. 1. Details of the repaired sample

122 After the drilling process, the hole edges and stitching area on the surface of each laminate was polished using

123 P400 abrasive paper. The samples were then cleaned with acetone to remove any residual dust. Carbon fibre

124 threads, based on 12K tows (supplied by Easy Composites, UK), were used in a hand-made stitching process.

125 Here, the number of the carbon fibre threads is corresponding to the diameter of the thread hole, which is 24K for

126 the hole of 1.5 mm in diameter, 72K for the hole of 2.5 mm in diameter and 144K for the hole of 3.5 mm in

127 diameter, respectively. The vacuum-assisted resin transfer moulding technique and infusion resin IN2 epoxy

(supplied by Easy composites, UK) was used to infuse the carbon fibre threads and bond the threads to the parent laminates. The samples were cured under vacuum at room temperature for 24 hours. The stitching, resin infusion process and the final sample are shown in Figs. 2(a) and (b). Fig. 2(a) shows the carbon fibre threads along the longitudinal direction of the sample, with each stitching step being carried out through the thickness of the repaired laminates in the scarf region. The green and yellow colour lines in Fig. 2(a) represent the carbon fibre threads. By using this stitching method, carbon fibre threads can be distributed symmetrically and uniformly on each side of the sample, as shown in Fig. 2(b). During the resin infusion process, the ends of carbon fibre threads were held in place using sticky tape. In Figure 2(b), there is a layer of peel ply on top of the repair patch, which is used to help compact and consolidate the repair. There is hardly any structural function of this surface layer, which is not shown in the schematic diagram.

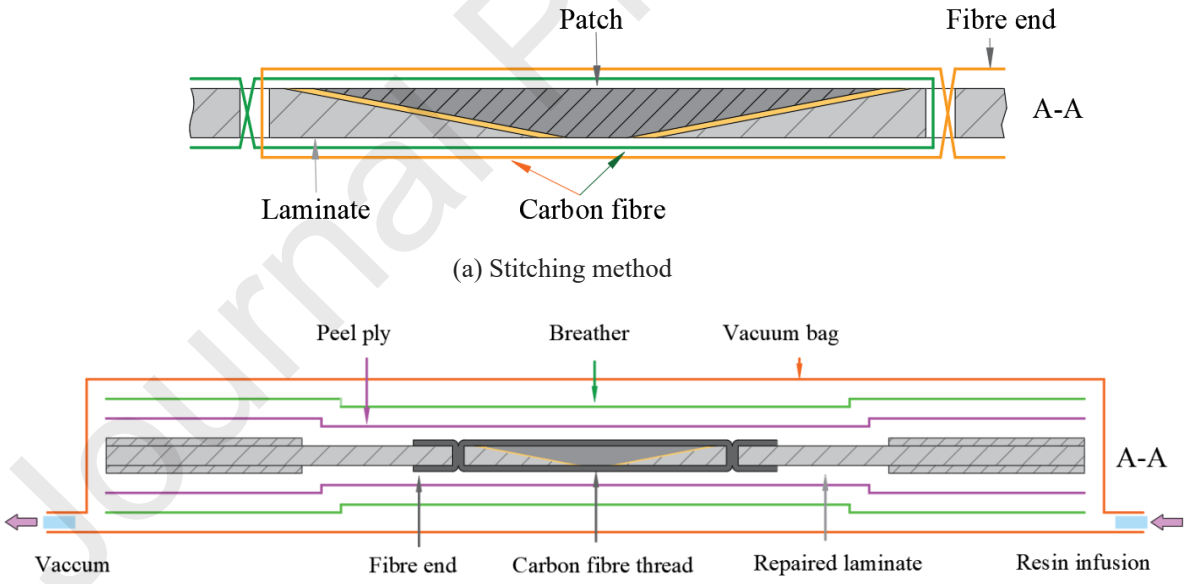


(a) Stitching method

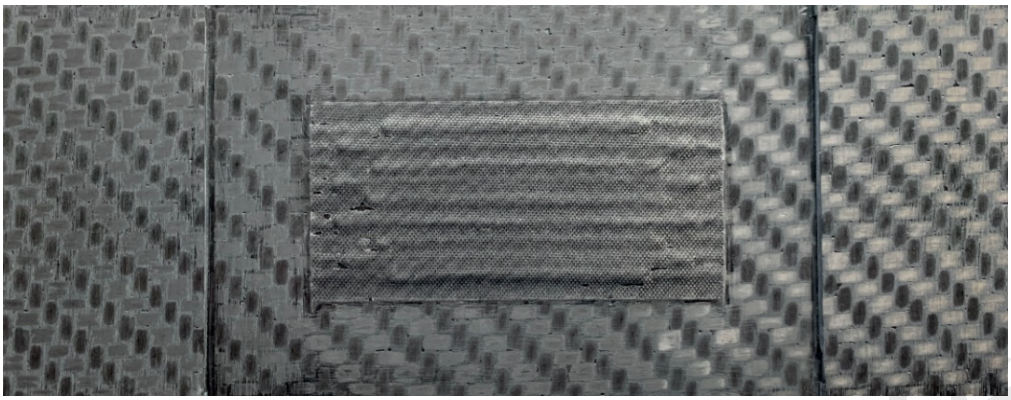

(b) Sample after curing

Fig. 2. Stitching procedure and the VARTM processes

The sample codes and geometrical details are listed in Table 1. To investigate the advantages of the stitching method, carbon fibre laminates based on a traditional scarf patch repair were also manufactures in order to provide a benchmark for the stitched repairs considered here. The sample codes DXX and HXX correspond to the diameters of repaired area and the threading hole respectively. For example, sample D48H1.5 represents a panel with a repair diameter of 48 mm and a threading hole diameter of 1.5 mm and sample D58 corresponds to an unstitched panel with a repair diameter of 58 mm.

Table 1. Geometrical details of samples

| Code of samples | Scarf ratio (Laminate thickness) | Diameter of thread holes (mm) |
|---|---|---|
| D48 | 1:8 | Unstitched |
| D48H1.5 | 1:8 | 1.5 |
| D48H2.5 | 1:8 | 2.5 |
| D48H3.5 | 1:8 | 3.5 |
| D58 | 1:10 | Unstitched |
| D58H1.5 | 1:10 | 1.5 |
| D58H2.5 | 1:10 | 2.5 |
| D58H3.5 | 1:10 | 3.5 |
| D68 | 1:12 | Unstitched |
| D68H1.5 | 1:12 | 1.5 |
| D68H2.5 | 1:12 | 2.5 |
| D68H3.5 | 1:12 | 3.5 |

The mechanical properties of XPREG XC130 and 12K carbon fibre are detailed in Table 2. As carbon fibre

laminates were made of woven prepreg, only the in-plane tensile strength and modulus along 0° were obtained according to the ASTM Standard D3039/D3039M-17 [18]. Poisson's ratio $\nu_{12}$ was obtained using this method. In addition, in-plane shear modulus and strength were calculated according to the ASTM Standard D3518/D3518M−18 [19]. The mechanical properties of 12K tow carbon fibre are provided by Easy Composites (UK).

Table 2. Mechanical properties of carbon fibre laminates and 12K tow carbon fibre.

| Carbon fibre laminates made of woven XPREG XC130 carbon fibre prepreg | |
|---|---|
| 0°/90° tensile modulus | 68 (GPa) |
| 0°/90° tensile strength | 997 (MPa) |
| Poisson's ratio $\nu_{12}$ | 0.13 |
| In-plane shear modulus $G_{12}$ | 14.5 (GPa) |
| In-plane shear strength $\tau_{12}$ | 60 (MPa) |
| **12K tow carbon fibre** | |
| 0° tensile modulus | 234 (GPa) |
| 0° tensile strength | 4830 (MPa) |

In Table 2, the subscript '1' and '2' in $\nu_{12}$, $G_{12}$ and $\tau_{12}$ are corresponding to the directions of 0° and 90° respectively.

### 2.2 Experimental Set-up and Procedure

The experimental set-up adopted for undertaking for the quasi-static tensile tests is shown in Fig. 3. Here, a 3D DIC rig was used to characterise the strain field across the sample. Before testing, random black and white speckles were introduced onto the sample surfaces using a spraying technique. After spraying, the pattern on samples was allowed to dry at room temperature for one hour, yielding a high quality surface with random speckles. The test sample was then clamped securely in the test machine, ensuring alignment between with the loading direction. Two XTDIC-CONST-SD cameras on tripods, supplied by XTOP 3D Technology (Shenzhen), were used to capture the 3D DIC measurements. In order to obtain high quality images of the sample, a uniform illumination was supplied by two LED light sources either side of the tripod. A calibration grid board was used to calibrate the position of the two cameras in order to capture strain field data at the repair location.

The samples were secured in serrated grips and loaded on an MTS 880 universal testing machine with a capacity of 333 kN. The crosshead displacement rate was set to 1 mm/min. and the resulting load and crosshead-displacement data were recorded on an associated workstation. Given the possibility of slippage occurring between the tabs and the grips during loading, the crosshead movement cannot be used to provide an accurate deformation response of the sample. Therefore, displacements over a 100 mm gauge length in the middle span of the sample were recorded using the DIC system. The strain field data and sample displacements within the gauge length were obtained using the 3D DIC software from XTOP 3D Technology.

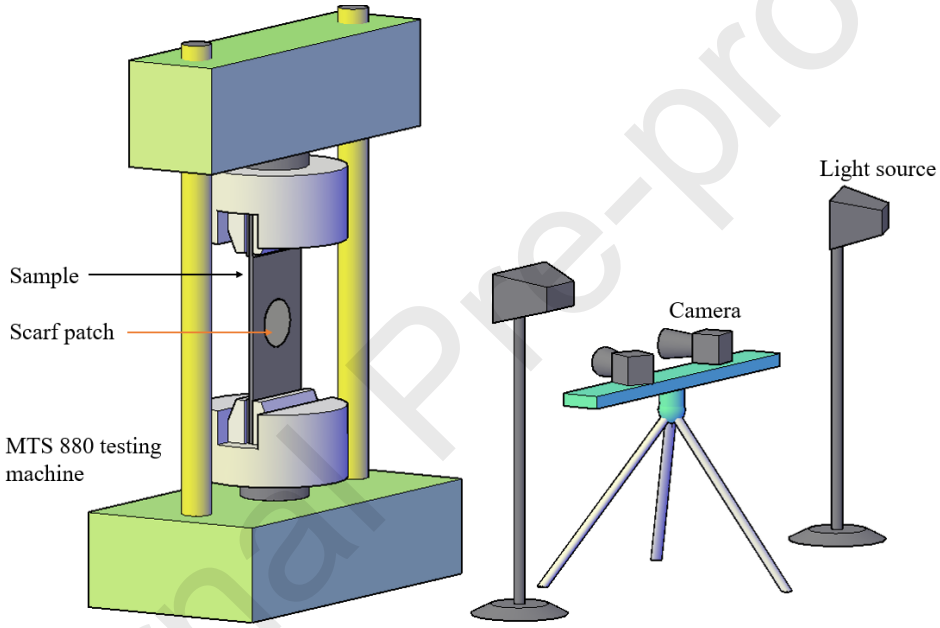


Fig. 3. Experimental set-up adopted for tensile testing.

## 3. Results and Discussion

### 3.1 Failure load

Fig. 4 compares the failure loads of the range of test samples presented in Table 1. It can be seen that for all sample groups, the failure load increases with increasing stitching hole size up to a value of 2.5 mm. This improvement in strength is due to the fact that the integrated carbon fibre threads share the load with the bonded area of the scarf joint. Clearly, there are greater numbers of fibres in samples with larger hole sizes, increasing the load-carrying capability of the joint. However, when the hole diameter reaches 3.5 mm, the failure load decreases quite significantly. Although the larger hole size has a greater number of fibres passing through it, the introduction of such a relatively large hole reduces the strength to values close to that of the unstitched laminate. There is clearly a balance between the benefits of incorporating greater numbers of fibres into the joint via larger holes and reducing the load-bearing capacity due to the larger hole size.

From Fig. 4, it can be seen that for the unstitched laminates, increasing the scarf ratio has little effect on the failure load over the scarf ratios of 1:8 and 1:10, with the exception being a small scarf ratio of 1:12, where the sample exhibited a 18 % reduction in failure load. Several observations have been made following the experimental investigations by Baig et al. [13] and Cheng et al. [17]. Baig et al. [13] noted that the sensitivity to the scarf ratio in a repaired laminate is linked to the manufacturing process used to produce the patch (pre-formed patch or prepreg patch) as well as the properties of the interface between the patch and the repaired area. It is evident in Fig. 4 that samples with a scarf ratio of 1:10 (Group-D58) exhibit the highest load-carrying capacity, whereas the failure loads for stitched samples with scarf ratios of 1:8 (Group-D48) and 1:12 (Group-D68) are similar. Cheng et al. [17] showed that the ultimate failure load is not only influced by the size of bonding area, but also by the load-carrying capacity of the parent material adjacent to the scarf jount. To achieve an optimum mechanical performance, an appropriate scarf ratio needs to be adopted. In the current study, as the width of all samples is

fixed at 100 mm, the influence of decreasing scarf ratio on the ultimate load is not significant, in general. However, in most cases, the effect of carbon fibre stiching is signicant. For example, relative to the unstitched laminates, the ultimate failure loads of the 2.5 mm stitched laminates increased by approximately 20, 27 and 45 % for scarf ratios of 1:8, 1:10 and 1:12, respectively.

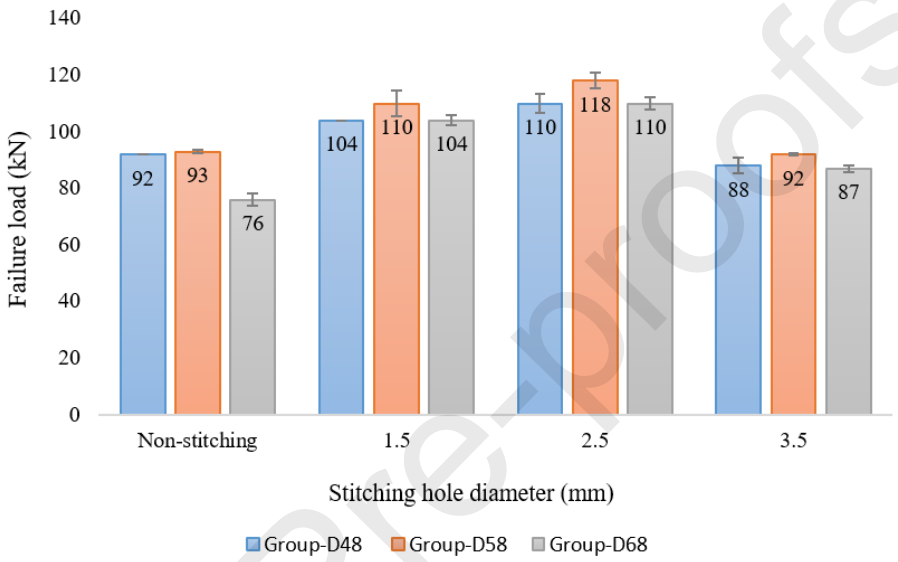


Fig. 4. Failure load comparison between different groups

### 3.2 DIC Analysis and Failure Mechanisms in Sample D58H2.5

From Fig. 4, it is clear sample D58H2.5 offers the highest ultimate tensile strength of all of the samples considered and this panel was selected for further investigation. Fig. 5(a) shows the longitudinal strain $\varepsilon_{yy}$ distribution (i.e. the strain in the loading direction) at loads corresponding to 35, 70 and 99 % of the ultimate value. Under these loading conditions, high strain regions can be seen at the tips of the stitching boundary. However, with increasing load, it is evident that while the strain values increase, the strain field patterns remain the same. Fig. 2(b) shows that the ends of stitching threads are bonded on the surface of laminate, and therefore high strains were detected there (Fig. 5a). From Fig. 5a, it can be clearly seen that relatively large strains occur at the stitch hole locations and around the top and bottom edges of the patch. The reason for this is that in these high strain areas, most of the load is transferred by the adhesive between the patch and the parent laminate, as well as carbon fibre stitches. Fig.

223 5(a) indicates that no significant change in strain is apparent in the carbon fibre threads away from the stitch hole,
224 with the strain remaining around 0.18 % until ultimate failure. This is due to the high strain areas mentioned above,
225 which support the loading-carrying capacity until final damage propagation, as shown in Fig. 5b. During the
226 loading process, any deformation along the loading direction of the repaired laminate region was constrained by
227 the carbon fibre threads. This evidence suggests that the ultimate strength is enhanced due to the stitches sharing
228 the load with the bonded patch.

229 For a traditional scarf patch repair, damage initiates from the edge of the patch and propagates laterally, as
230 shown for laminate D48 in Fig. 7. In Fig. 5(b), in contrast to the traditional scarf patch repaired laminates, no
231 damage was found at the edge of the patch. Damage initiated from the thread holes in the lower part of the repaired
232 laminates and propagated towards the laminate edges, whilst the upper part of the stitched area remained intact.
233 Damage also initiated in the upper part of the repaired region, due to the symmetric nature of the repaired laminates.
234 Damage initiated due to the stress concentration around the hole and the patch edge, close to the boundary of the
235 stitching area, as shown in Fig. 5b. Further, deformation at the patch edge, near the stitching boundary, is not
236 effectively constrained by the carbon fibre threads. As the result, damage initiation occurs at this location. In a
237 perfect laminate, damage can initiate from any of the four holes close to edges of the laminate. In practice, due to
238 imperfections introduced during the manufacturing processes and test set-up, damage starts from the weakest of
239 the four holes and propagates along the x-axis towards the edge of the laminate.

240 To conclude, in order to achieve the best tensile strength, both the scarf angle and the stitching hole size should
241 be optimised. For a given width of a laminate, as the scarf patch size is increased, greater amounts of parent
242 material need to be removed in the repairing process. As a result, there will be less parent material on either side
243 of the bonded area across the x-axis direction, with the effect that lower levels of load will be transferred by the
244 parent material. On the other hand, as a result of the carbon fibre stitching, the bonding area is well protected and

damage initiates from the critical threading hole. Therefore, the hole size becomes crucial, affecting the tensile strength of the repaired laminate. Based on the current work, a combination of a 2.5 mm hole diameter and a scarf ratio of 1:10 appears most appropriate.

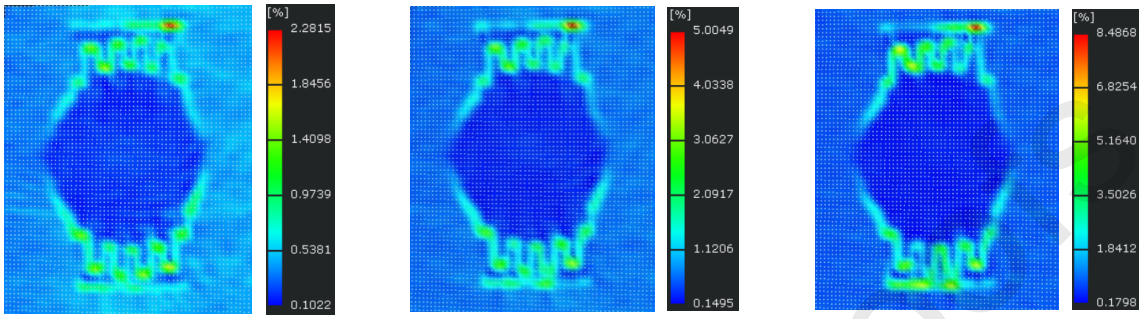


35 % of failure load 70 % of failure load 99 % of failure load

(a) Development of $\varepsilon_{yy}$ at different loading levels

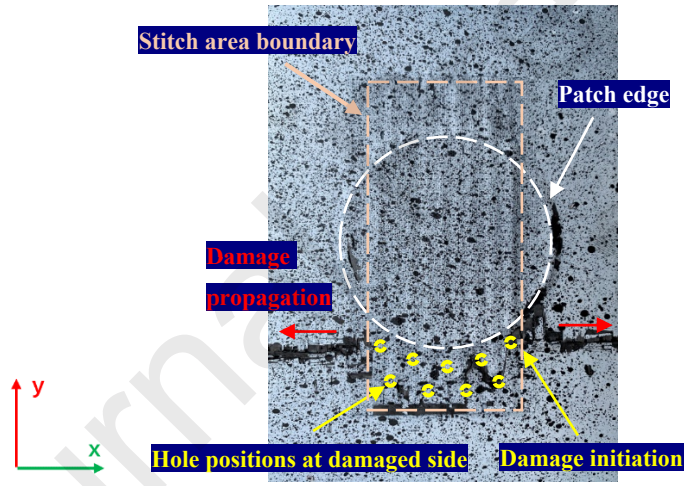


(b) Failure mode

Fig. 5. DIC results and failure mode of D58H2.5

### 3.3 DIC analysis of the influence of stitching hole diameter on failure mechanisms

The DIC results show that for a given scarf ratio, the effect of stitching hole diameter on load-carrying capacity is similar. Thus, for simplification the attention will focus on the Group-D48 laminates.

253 Fig. 6 shows the development of the strain $\varepsilon_{yy}$ field in the D48 samples in the loading direction. For the sample
254 without stitches (D48), i.e. a traditional single-sided scarf patch repair, the maximum strain occurs at the edges of
255 the patch along the y-axis (in the loading direction) for all loading conditions prior to the onset of failure. However,
256 the strain value is small at the edges of the patch along the x-axis. This is due to debonding initiation at the upper
257 and lower edges of the patch along the y-axis, as the load is primarily transferred by the adhesive.
258 For the sample with 1.5 mm stitches (D48H1.5), the strain field is more dispersed than in the traditional scarf
259 patch laminate (D48), although there are some regions of high strain occurring at higher loads at the holes close
260 to the upper and lower patch edges. This is attributed to the 1.5 mm diameter stitching holes, which result in the
261 load being more broadly distributed in the repaired region. As the result, the strain values in the upper and lower
262 regions of the patch edge were reduced, with the effect that damage at the adhesive interface between the scarf
263 patch and the parent laminate was postponed. This is reflected in a higher failure load (increasing from 92 kN to
264 104 kN, Fig. 4). For the samples with 2.5 mm (D48H2.5) and 3.5 mm (D48H3.5) hole diameters, the corresponding
265 strain fields follow the stitch pattern with high strain regions being observed at the stitching tips and low strain
266 values below the scarf patch. There is a further increase in the failure load, i.e. from 104 kN for D48H1.5 to 110
267 kN for D48H2.5. However, with a further increase in the hole size to 3.5 mm, the failure load reduces from 110
268 kN to 88 kN, this being attributed to the very high local strains at the top stitching tips (D48H3.5). Here, there is
269 a high strain (and therefore stress) concentration, with damage being shown by black regions in the strain plots.
270

D48

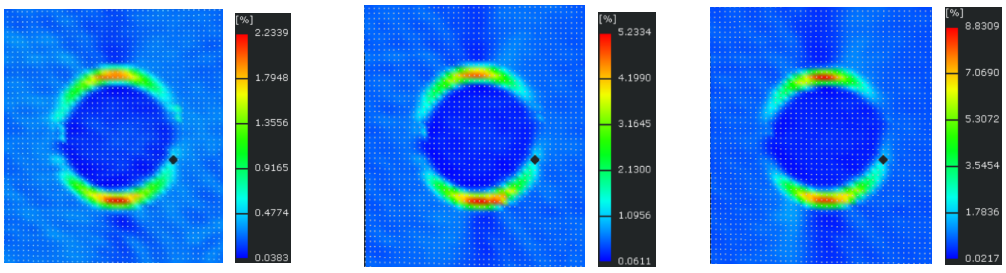

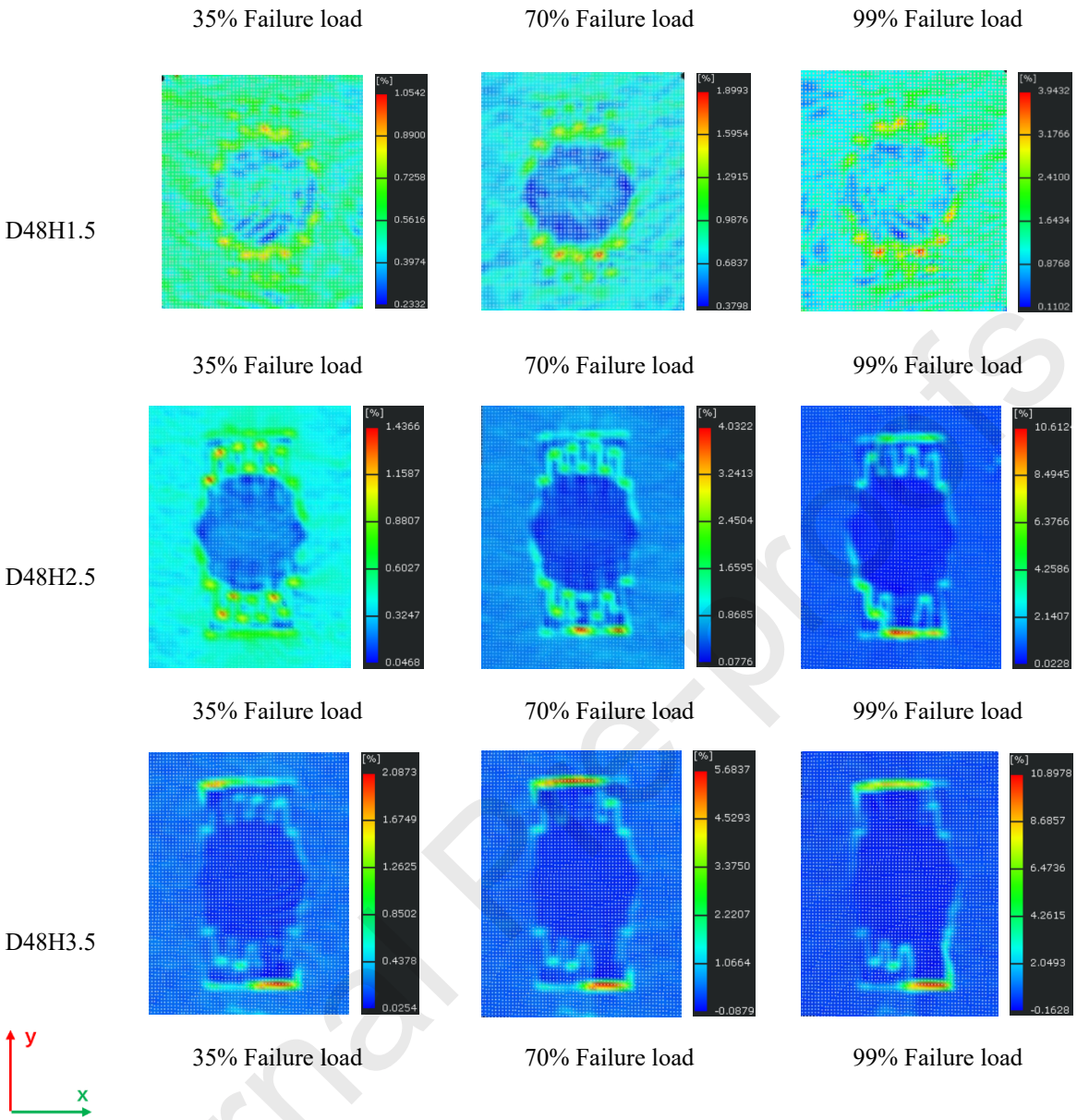


271 Fig. 6. Development of the $\varepsilon_{yy}$ strain field in Group-D48 samples at different loading levels.

272

273 Figure 7 shows the failure modes in the D48 family of samples. For the sample without any reinforcing
274 stitches (D48), damage initiates at the upper edge of the interface between the scarf patch and the parent laminate
275 and then propagates towards the edges of the parent laminate, as a result of debonding of the interface. This
276 ultimately results in complete failure of the test panel. Failure in the sample with 1.5 mm diameter stitching holes
277 (D48H1.5) shifts to the edge of the patch, close to the boundary of the stitched area. Here, the white circle
278 represents the position of the scarf patch and the pink rectangle represents the boundary of the stitched area.

Damage initiation from the edge of the patch in the y-axis direction is constrained by the stitching fibres. However, for the area beyond the boundary of the stitched area, damage initiation is relatively limited. For the samples with larger stitching holes, i.e. D48H2.5 and D48H3.5, damage initiates from the hole which is closest to the edge of the laminate. From Fig. 7, no damage was observed within the stitching boundary for laminates D48H2.5 and D48H3.5. This evidence indicates that the failure mode observed in laminates D48H2.5 and D48H3.5 are different to those identified in D48H1.5.

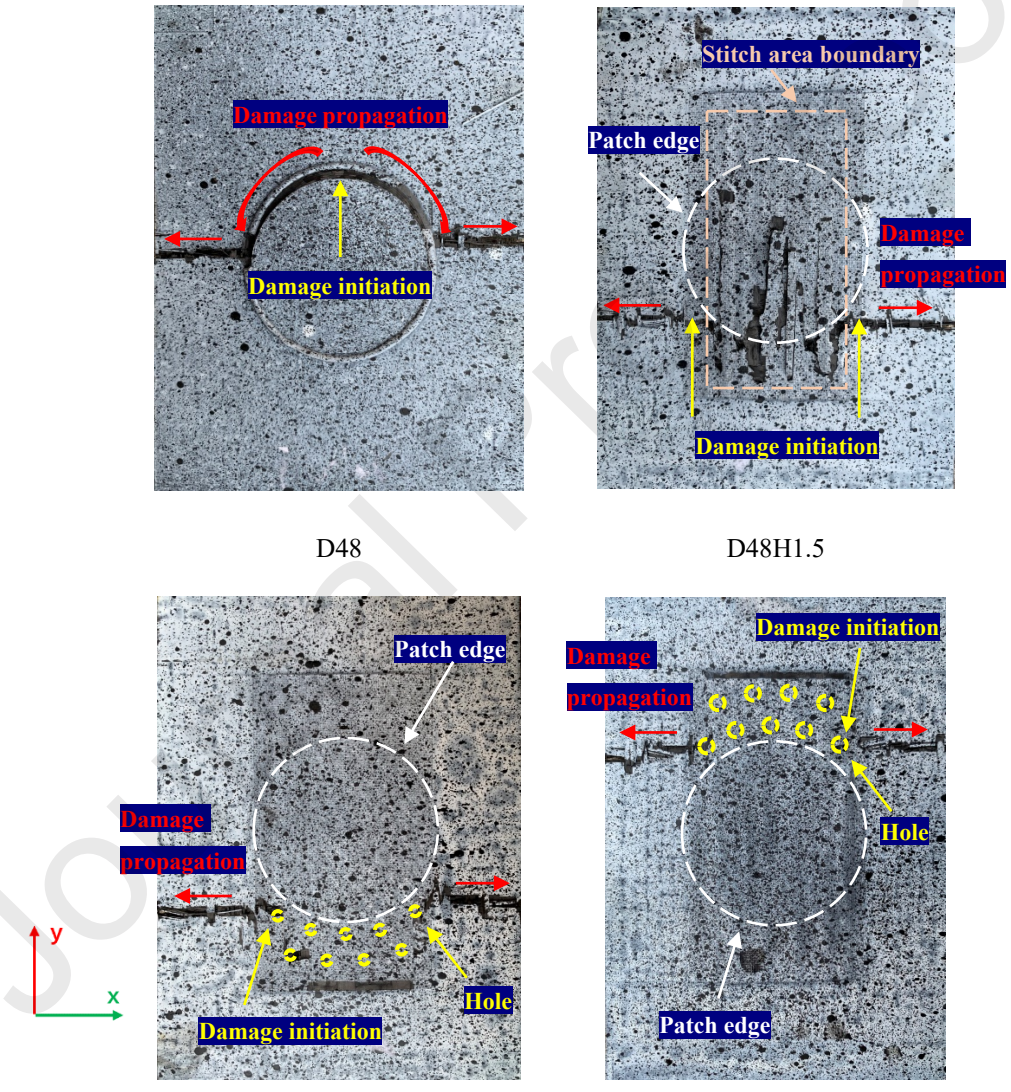


D48 D48H1.5

D48H2.5 D48H3.5

Fig. 7. Failure modes of Group-D48 samples

In summary, the failure mechanisms observed in laminates containing carbon fibre stitches are significantly

different to those seen in traditional scarf patch repaired laminates. When the hole diameter is below 2.5 mm, the fibre threads are not sufficiently strong to constrain the deformation of the patch and prevent damage initiation at the edge of the patch. However, when the hole size is greater than 2.5 mm, the bonding area associated with the scarf is well protected during loading. Here, the hole size plays an important role in determining the failure mode (and strength) of the repaired laminate, since the regions around the edges of the hole become weak, triggering damage initiation.

### 3.4 DIC analysis of the influence of scarf ratio on failure mechanisms

Considering the traditional scarf-repaired laminates D48, D58 and D68 in Fig. 4, the scarf ratio has some influence on the tensile strength of the samples. However, the results show that the scarf ratio has little effect on the failure mechanisms observed in these conventionally-repaired laminates. The failure mechanisms observed in samples D58 and D68 are similar to sample D48, shown in Fig. 7.

Regarding the stitched samples, varying the scarf ratio has a similar effect on the load carrying-capacity of samples (Fig. 4). Therefore repaired laminates based on a 1.5 mm hole diameter are considered in the following. Fig. 8 shows the strain field for samples D48H1.5, D58H1.5 and D68H1.5, corresponding to scarf ratios of 1:8, 1:10 and 1:12 respectively. It is clear that the larger the patch size, the greater the measured strain. It is also clear that there are low strain regions in the scarf patches for all three scarf ratios, due to the fact that the carbon fibre stitches carry a large percentage of the load. The regions of highest strain are found around the threading holes along the stitching boundary. These values increase with decreasing scarf ratio, being approximately 3 % for D48H1.5, 5 % for D58H1.5 and 6 % for D68H1.5. This is due to the fact that as the patch size increases, the volume of residual parent material decreases, introducing regions of large deformation around the stitching holes along the upper and lower patch boundaries (Fig. 8). In addition, when the stitch size remains constant in Fig. 8,

309 the carbon fibre tows apply less constraint in samples based on larger scarf patches. Figure 9 shows the failure
310 modes in samples D58H1.5 and D68H1.5. As was the case in sample D48H1.5 shown in Fig. 7, damage initiates
311 from the edge of the patch, outside the stitching area and propagates horizontally towards the edges of the laminate.
312 This evidence suggests that the scarf ratio appears to have a limited effect on the failure modes in the stitched
313 laminates.

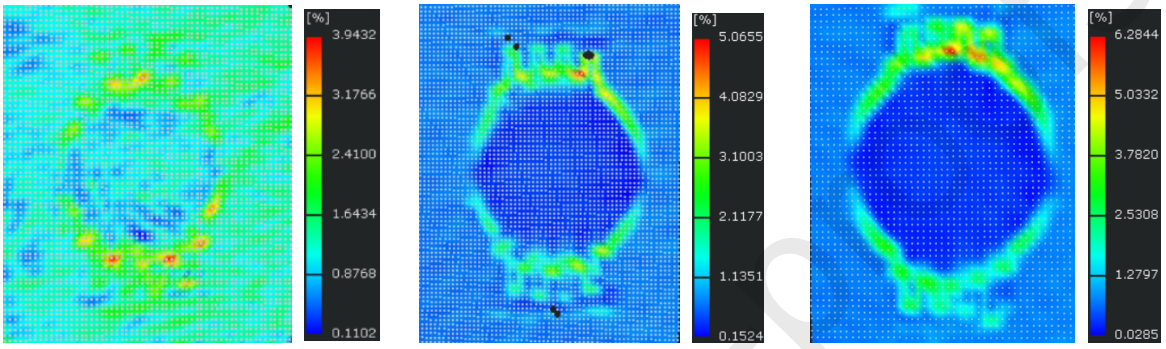


D48H1.5 D58H1.5 D68H1.5

314 Fig. 8. $\varepsilon_{yy}$ strain distribution in panels D48H1.5, D58H1.5 and D68H1.5 close to the failure load.

315

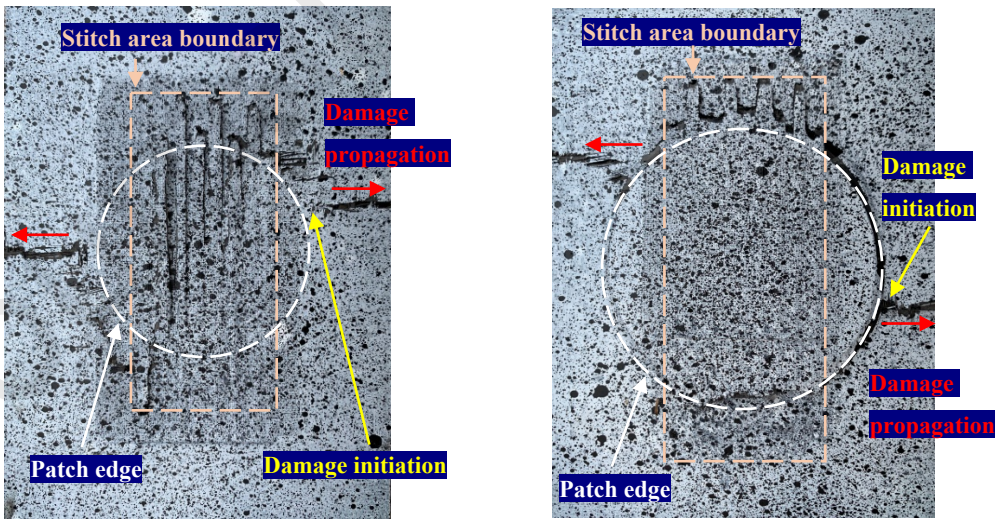


D58H1.5 D68H1.5

316 Fig. 9. The failure modes in Panels D58H1.5 and D68H1.5.

317

## 4. Conclusions

In this paper, an innovative composite repair technology has been developed to demonstrate the effectiveness of localised carbon fibre stitching on the mechanical performance of scarf-repaired composite laminates. Here, the influence of stitch size and scarf ratio on the load-carrying capacity of repaired composite laminates has been studied. Based on the findings of this research study, the following conclusions can be drawn:

(1) Repaired laminates with a stitching hole size of 2.5 mm and a scarf ratio of 1:10 offered the highest failure load (118 kN), a value that is 28 % higher than its non-stitched counterpart, having the same scarf ratio. The mechanical performance of a stitch-repaired carbon fibre laminate is dependent on the scarf patch size and stitch size. If the former is too large there is less parent material for a given panel width, which negatively impacts the strength of the repaired laminate. If the hole size is too large, the strength of the panel is reduced, due to the reduced cross-sectional area. Therefore, there is a balance between scarf patch size and thread hole size.

(2) The stitch size influences the failure mechanisms observed in the repaired laminates. When the hole diameter is below 2.5 mm, damage initiates from the scarf patch outside the stitching boundary. When the hole diameter is above 2.5 mm, damage initiates from the hole close to edge of the laminate.

(3) The scarf ratio has a limited effect on the failure load and failure mechanisms observed in the repaired laminates. However, in terms of load-carrying capacity, a scarf ratio of 1:10 has been shown to be the most appropriate of those considered here.

The current research is an exploration on an innovative stitch-reinforced scarf patch, together with the vacuum resin infusion, for composite repair. Unitil now, the laminates repaired is only reinforced in the longitudinal (loading) direction. However, the stitch-reinforced technology developed can be broadened to strengthen the reparied panel in other directions by designing an appropriate stitching pattern, which provides a scope for futhre work.

**Data availability**

The raw/processed data required to reproduce these findings cannot be shared at this time as the data also forms part of an ongoing study.

**References**

[1] Liu, X. and Wang, G., 2007. Progressive failure analysis of bonded composite repairs. *Composite Structures*, *81*(3), pp.331-340.

[2] Andrew, J.J., Arumugam, V., Bull, D.J. and Dhakal, H.N., 2016. Residual strength and damage characterization of repaired glass/epoxy composite laminates using AE and DIC. *Composite Structures*, *152*, pp.124-139.

[3] Kradinov, V., Hanauska, J., Barut, A., Madenci, E. and Ambur, D.R., 2002. Bolted patch repair of composite panels with a cutout. *Composite structures*, *56*(4), pp.423-444.

[4] Her, S.C. and Shie, D.L., 1998. The failure analysis of bolted repair on composite laminate. *International journal of solids and structures*, *35*(15), pp.1679-1693.

[5] Park, S.S., Choe, H.S., Kwak, B.S., Choi, J.H. and Kweon, J.H., 2018. Micro-bolt repair for delaminated composite plate under compression. *Composite Structures*, *192*, pp.245-254.

[6] Kang, G.S., Kwak, B.S., Choe, H.S. and Kweon, J.H., 2019. Parametric study on the buckling load after micro-bolt repair of a composite laminate with delamination. *Composite Structures*, *215*, pp.1-12.

[7] Kashfuddoja, M. and Ramji, M., 2013. Whole-field strain analysis and damage assessment of adhesively bonded patch repair of CFRP laminates using 3D-DIC and FEA. *Composites Part B: Engineering*, *53*, pp.46-61.

[8] Liu, X. and Wang, G., 2007. Progressive failure analysis of bonded composite repairs. *Composite Structures*, *81*(3), pp.331-340.

[9] Gong, X.J., Cheng, P., Rousseau, J. and Aivazzadeh, S., 2007, July. Effect of local stresses on static strength and fatigue life of patched composite panels. In *16th International Conference on Composite Materials* (pp. 8-13).

[10] Cheng, P., Gong, X.J., Hearn, D. and Aivazzadeh, S., 2011. Tensile behaviour of patch-repaired CFRP laminates. *Composite structures*, *93*(2), pp.582-589.

[11] Kashfuddoja, M. and Ramji, M., 2013. Whole-field strain analysis and damage assessment of adhesively bonded patch repair of CFRP laminates using 3D-DIC and FEA. *Composites Part B: Engineering*, *53*, pp.46-61.

[12] Hamoush, S., 2004. *Failure analysis and surety design of composite patching systems* (No. SAND2004-4083). Sandia National Laboratories.

[13] Baig, Y., Cheng, X., Hasham, H.J., Abbas, M. and Khan, W.A., 2016. Failure mechanisms of scarf-repaired composite laminates under tensile load. *Journal of the Brazilian Society of Mechanical Sciences and Engineering*, *38*(7), pp.2069-2075.

[14] Pinto, A.M.G., Campilho, R.D.S.G., De Moura, M.F.S.F. and Mendes, I.R., 2010. Numerical evaluation of three-dimensional scarf repairs in carbon-epoxy structures. *International Journal of Adhesion and Adhesives*, *30*(5), pp.329-337.

[15] Bendemra, H., Compston, P. and Crothers, P.J., 2015. Optimisation study of tapered scarf and stepped-lap joints in composite repair patches. *Composite Structures*, *130*, pp.1-8.

[16] Wang, C.H. and Gunnion, A.J., 2008. On the design methodology of scarf repairs to composite laminates. *Composites Science and Technology*, *68*(1), pp.35-46.

[17] Cheng, X.Q., Baig, Y., Renwei, H., Yujian, G. and Jikui, Z., 2013. Study of tensile failure mechanisms in scarf repaired CFRP laminates. *International Journal of Adhesion and Adhesives*, *41*, pp.177-185.

[18] ASTM standard D3039/D3039M-17 (Standard Test Method for Tensile Properties of Polymer Matrix Composite Materials)
[19] ASTM Standard D3518/D3518M−18 (Standard Test Method for In-Plane Shear Response of Polymer Matrix Composite Materials by Tensile Test of a ±45° Laminate)

Author statement

C. Sun: Data curation, Writing- Original draft preparation. W. Zhao: Data curation. J. Zhou: Visualization, Investigation. M. Altenaiji: Writing-Reviewing and Editing. W.J. Cantwell: Writing- Reviewing and Editing. Z.W. Guan: Conceptualization, Methodology, Supervision

## Highlights

- An innovative composite repair technology with a stitched scarf panel
- Significant enhancement on load carrying capacity of the repaired laminates
- There is a balance between scarf patch size and thread hole size
- The scarf ratio has a limited effect on the failure load and failure mechanisms
- Repaired laminate with 2.5 mm stitch size and 1:10 scarf ratio offer the highest failure load